

# Surface chemistry of the lung surfactant system: Techniques for *in vitro* evaluation

R. Banerjee

Biomedical Engineering, Indian Institute of Technology-Bombay, Powai, Mumbai 400 076, India

**Our lungs are lined by a surface-active material which is responsible for lowering surface tension to near zero values on expiration, and preventing lung collapse. The presence of a functional lung surfactant reduces the work of breathing. Respiratory Distress Syndrome (RDS) is a disease due to lack of lung surfactant in pre-term babies (born before nine months). Surfactant dysfunction also occurs in many adult respiratory diseases like adult respiratory distress syndrome, asthma and chronic bronchitis. The surface properties of surfactants are important factors, which determine their suitability for exogenous therapy in conditions of surfactant dysfunction. Various *in vitro* techniques, commonly used in surface science, are modified to suit them for application to the lung surfactant system – for study of the surface properties of surfactants under dynamic conditions, which simulate those present *in vivo* in the pulmonary system. This paper outlines some of these techniques as applied to the lung surfactant system and discusses the relevance of surface properties to pulmonary physiology.**

OUR lungs have a thin liquid lining with a complex surface-active material called pulmonary surfactant, forming a film at the air–aqueous interface. In 1929, von Neergaard first attributed the difference in the recoil forces between fluid- and air-filled lungs to the action of surface tension, characteristic of an air–aqueous interface. Pulmonary surfactant is a complex mixture of lipids and surfactant-specific proteins synthesized by specialized type II cells in the lungs. Lung surfactant reduces surface tension at the air–aqueous interface of the terminal respiratory units (alveoli), prevents them from collapsing during expiration and reduces the work of breathing (see Table 1). This review gives a brief description of the surface chemistry of this unique biological system and discusses the methods used for improving our understanding of its functions.

## Surfactant composition

Pulmonary surfactant is composed of approximately 90% lipids and 10% proteins<sup>1</sup>. Figure 1 depicts the dis-

tribution of lipids and proteins in lung surfactant. More than 85% of the surfactant lipid is phospholipid, whereas cholesterol is the most abundant neutral lipid component. Phosphatidylcholine (PC) represents 70 to 80% of the surfactant phospholipid fraction and approximately 60% of it is fully saturated. This saturated PC is mainly dipalmitoyl phosphatidylcholine (DPPC). Phosphatidylglycerol (PG) is the second most abundant phospholipid in the surfactant accounting for almost 10% of the total surfactant composition. There are four surfactant-specific proteins, namely SP-A, SP-B, SP-C and SP-D, which play a role in the optimal functioning of the surfactant.

DPPC is the main component responsible for the surface tension reduction. A surface monolayer highly enriched in DPPC is responsible for the critical reduction in surface tension to values near zero, on compression of the monolayer (during expiration).

## Role of surfactant function in pulmonary physiology

The five most important surface properties of the surfactant system which are essential for normal lung function are (1) rapid film formation by adsorption of surface-active material from the hypophase; (2) achieving near-zero surface tensions on film compression; (3) low film compressibility, which allows achievement

**Table 1.** Role of surfactant in the lungs

Terminal units of lungs: spherical alveoli
Pulmonary surfactant lines alveoli and reduces surface tension
Near zero surface tension prevents collapse of lungs during expiration

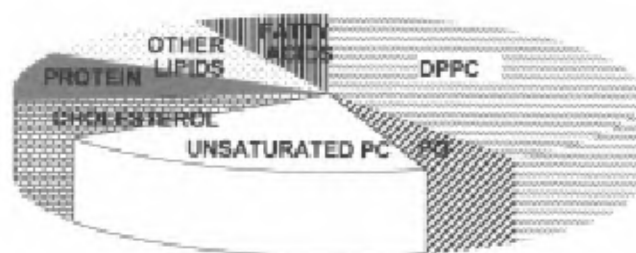
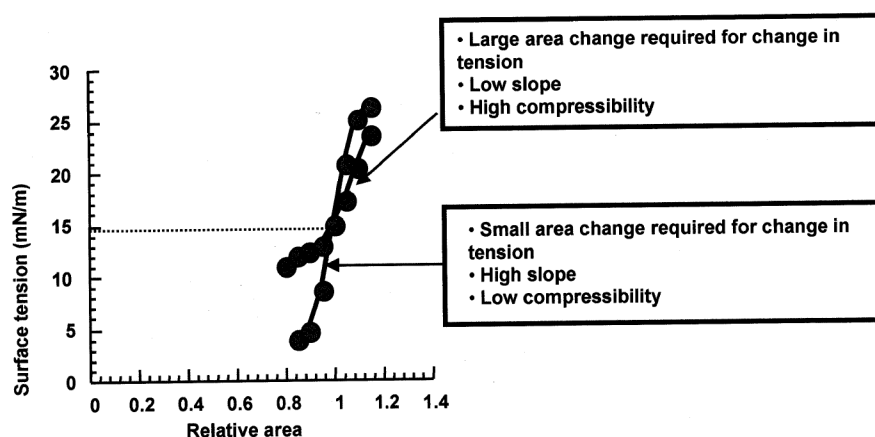


**Figure 1.** Composition of pulmonary surfactant.

e-mail: rint@iitb.ac.in



Compressibility at 15 mN/m =  $dA/d\gamma/A$ , where  $A$  is the area at 15 mN/m,  $\gamma$  is the surface tension and  $(dA/d\gamma)$  is the inverse of the slope of the isotherm at 15 mN/m

Figure 2. Calculation of compressibility.

Table 2. Properties of an effective lung surfactant

Achieves <i>low minimum surface tension</i> on compression (< 10 mN/m); Prevents collapse during expiration
<i>Quick adsorption</i> to a surface tension of ~25 mN/m
<i>Low compressibility</i> : Less of an area change required for low surface tension; Large area left in lungs for gas exchange
<i>High stability</i> : Surfactant is stable at a low tension and film does not collapse
<i>High re-spreading</i> : Ability to re-enter the interface and be replenished with many breaths

of a near-zero surface tension on minimal compression of the film; (4) a stable film which can maintain low surface tensions over many minutes to hours; and (5) effective replenishment of the surface film during expansion by incorporation of surfactant to the interface (see Table 2).

Film compressibility is a property, which denotes the inverse of the slope of the isotherm of lung surfactant. Its calculation is explained in Figure 2. The lower the compressibility, the more beneficial is the surfactant as less of an area change is then required for reduction of surface tension, leaving a large surface area behind in the lungs for gas exchange.

The Laplace law states that the pressure required to distend a sphere is directly proportional to the surface tension at the spherical interface and inversely proportional to the radius of the sphere. Hence, as the spherical alveoli in the lungs reduce in size during expiration, there is a decrease in their surface area and the surface tension tends to increase<sup>2</sup>. A smaller alveolus always requires a higher internal pressure than a larger alveolus, to maintain or expand its size. The unique ability of lung surfactant to decrease the surface tension of the interface during expiration and increase the surface tension during inspiration, helps in stabilizing alveoli of different sizes in the lungs.

Table 3. Surfactant dysfunction in respiratory diseases

Respiratory distress	: Neonatal Respiratory Distress Syndrome Adult Respiratory Distress Syndrome
Airway diseases	: Asthma Chronic bronchitis
Infective conditions	: Tuberculosis Influenza Pneumonias
Occupational diseases	: Coal worker's lungs Silicosis
Toxic hazards	: Gas poisoning Smoking Air pollution
Cancer	: Lung carcinoma

During normal respiration, there is a change in lung surface area from the total lung capacity to the functional residual capacity – a 54% area reduction<sup>3</sup>. Clements *et al.*<sup>4</sup> proposed that the alveolar surface tension was < 10–15 mN/m and was unstable when the surfactant film was maximally compressed. Advances in our knowledge of the lung surfactant system have allowed *in vivo* measurement of surface tension in the lungs and have shown that lung surfactant reaches surface tensions near zero with 15–20% area compression.

### Clinical consequences

If the amount or quality of lung surfactant is inadequate, or the surfactant present is inactivated, the work of breathing increases in order to re-expand the alveoli with each breath and permit adequate gas exchange. One such condition is the Neonatal Respiratory Distress Syndrome (RDS), which is due to a deficiency in lung surfactant in pre-term babies (born before nine months)<sup>5–7</sup>. Many adult respiratory diseases like adult respiratory distress syndrome and lung injury also have a dysfunctional surfactant system due to inactivation of the surfactant (see Table 3). By providing the necessary

reductions in alveolar surface tension, an exogenous surfactant will, in principle, improve gas exchange and minimize lung injury in all conditions of surfactant deficiency and/or dysfunction.

The presence of pulmonary surfactant reduces the work of breathing – 2% of the total energy is utilized for breathing in the presence of surfactant, whereas in its absence this increases to 33% of the total energy.

### Role of surfactant in adult respiratory diseases

Lung surfactant is adversely affected in many respiratory conditions; a few common examples are mentioned in this section. Perhaps, adequate replacement can alleviate some of these problems.

Surfactant is known to line our airways. Major functions proposed for surfactant in the airways are to maintain patency of terminal and conducting airways, and to prevent liquid and mucus plugging. Perhaps the high surface pressures generated by surfactant squeeze liquid out of the airway and provide a physical force to oppose airway collapse. This concept is supported indirectly by both animal and clinical studies. Administration of exogenous surfactant to the lungs of sensitized guinea pigs significantly diminished allergen-induced bronchoconstriction<sup>8</sup> and a beneficial effect of surfactant therapy has been preliminarily reported in acute asthma<sup>9</sup>.

In a study by Anzueto *et al.*<sup>10</sup>, aerosolized surfactant improved pulmonary function and resulted in a dose-related improvement in sputum transport by cilia in patients with stable chronic bronchitis.

In tuberculosis, there is evidence of decompensation of the lung surfactant system with impairment in the morphological organization, biochemical composition and surface-active properties<sup>11</sup>.

The effect of pulmonary surfactant treatment in cases of smoke inhalation and carbon monoxide poisoning was studied by Xie *et al.*<sup>12</sup> in rat models. Significant improvements were observed in the surface tension properties of bronchoalveolar lavage fluid, static lung compliance and the oxygenation on exogenous surfactant treatment.

Surfactant proteins play an important role in enhancing the surface properties of pulmonary surfactant and participate in host-defense mechanism(s) of the lungs. A selective reduction in SP-B content was found following chronic exposure to cigarette smoke and suggests an inhibitory effect of cigarette smoke on surfactant secretory processes and/or a localized destruction of surfactant proteins on the bronchoalveolar surface<sup>13</sup>.

Air pollutants like ozone, nitrogen dioxide, diesel exhaust, silica and asbestos cause a structural alteration of lung surfactant, leading to an impairment of the biological activity of both surfactant phospholipids and surfactant-specific proteins<sup>14</sup>.

On comparing the phospholipids of the lung cancer locus, surroundings tissues, and pulmonary surfactant obtained from these sites, the level of PG in all histological forms of lung cancer, irrespective of the stage of malignant process in tumour locus, was almost twice as less compared both to the normal lung tissue and non-malignant tissues<sup>15</sup>. These results point to impaired PG metabolism of the bronchopulmonary system in lung cancer.

### *In vitro* evaluation of surfactants for RDS

The surface properties of surfactants are important factors, which determine their suitability for exogenous therapy. Various *in vitro* techniques commonly used in surface science are modified to suit them for application to the lung surfactant system – for study of the surface properties of surfactants under dynamic conditions which simulate those present *in vivo* in the pulmonary system.

#### Langmuir–Blodgett trough (Wilhelmy balance)

The Langmuir–Wilhelmy surface balance was introduced by Clements in 1957 (ref. 16), to investigate surfactant films in his pioneering work on the lung surfactant system. The instrument allows for the compression of monolayers under constant speed, to a target surface pressure and also allows the monolayer film to be held at constant surface pressure, while other parameters are adjusted.

The area of the surface film is changed by mechanically moving the barriers. The surface pressure is monitored. Surface pressure ( $\pi$ ) is  $\gamma_0 - \gamma$ , where  $\gamma_0$  is the surface tension of the clean surface and  $\gamma$  is surface tension with surfactant present.  $\pi$  is thus the amount by which the surfactant lowers surface tension.

This instrument is based on the principle of Rayleigh's equation:

$$\pi A = \text{constant}, \quad (1)$$

where  $A$  is the area of the film. Thus, as the area is decreased the film pressure rises and these changes are noted on compression and expansion of the monolayer.

The subphase is filled with a substance having a composition similar to that of the fluid lining the lungs. Foetal lung fluid, when compared with plasma, has high  $K^+$ ,  $H^+$  and  $Cl^-$ , low  $Ca^{2+}$  and  $HCO_3^-$ , and a similar amount of  $Na^+$  (ref. 17). Use of buffered solutions containing calcium and having a pH of 7.4 would simulate the lungs more effectively<sup>18</sup> than a subphase of distilled water.

The barriers are cycled at high speeds in order to simulate the breathing cycle and all experiments are

carried out at body temperature of 37°C. Seeger *et al.*<sup>19</sup> have used barrier speeds of 2.5 min/cycle and Tabak and Notter<sup>20</sup> have used 400 s/cycle. The Wilhelmy balance does not allow as high compression speeds as other dynamic methods of surface tension evaluation, like the pulsating bubble surfactometer. Figure 3 shows a schematic representation of a Langmuir trough with the main modifications required for its use in the lung surfactant system.

The surfactant to be studied can be spread on the air–aqueous interface or can be dissolved in the subphase, and allowed to equilibrate to the surface. Surfactants can be spread on the air–aqueous interface either as a dry powder<sup>21</sup> or as drops of a solution using a water immiscible organic solvent as a vehicle. This latter technique has been most commonly used in studies of the pulmonary surfactant system and was first described by Phillips and Chapman<sup>22</sup>. This method has the advantage of convenience, but time must be allowed for evaporation of the solvent and precautions must be taken so that all traces of the solvent are removed, in order to avoid erroneous results. Besides, adsorbed films occur in the lungs *in vivo*, surfactant adsorbs to the interface from the alveolar hypophase, on taking a deep breath.

The extent to which the expanded film of surfactant is compressed varies in the different studies. Based on calculations of tidal volumes and functional residual volumes in the lungs, Hills *et al.*<sup>23</sup> have suggested that compression ratios up to a maximum of 2.87 : 1 should be used for simulation of pulmonary conditions. Most studies however, have used much higher compression ratios. Though these higher ratios do not simulate the lung conditions, they yield maximum information regarding the collapse of surfactant films and the ability of surfactants to re-spread from the hypophase to the interface.

### Advantages and disadvantages

This apparatus is well suited for examining surface-tension area characteristics for films having surface tensions between 70 mN/m, observed for a clean saline surface at 37°C and the equilibrium surface tension for phospholipids, ~ 25 mN/m. However, on lateral compression of insoluble films to cause a decrease in surface tension below the equilibrium state, the previously hydrophobic top edges of the trough become wetted by the film plus aqueous solution and the solution overflows.

Another problem is that of the contact angle on the Wilhelmy plate. The Wilhelmy method relies on the continual presence of a zero contact angle between the vertical dipping plate and the surface of the fluid within the trough. At high surface pressures the meniscus on the plate decreases, often leaving behind a film of lipid

material; upon re-expansion of the monolayer, the liquid meniscus must re-spread and advance upward to attract the Wilhelmy plate, which does not always happen.

At low surface tensions, surfactant molecules can spread easily at the Teflon–water interface, resulting in leakage past the surface barrier. Goerke and Gonzales<sup>24</sup> dealt with the leakage problem by priming the Teflon barrier and walls with long-chain saturated PC and a solution of lanthanum, thus rendering the Teflon walls hydrophilic.

Large volumes are required, and the barrier cannot be cycled very quickly, as it creates waves. These disadvantages make the Wilhelmy balance less suitable than the surfactometers in most studies of adsorbed model lung surfactant systems. However, this system is well suited for studying solvent-spread films in which precise amounts of film material can be deposited at the interface, surface radioactivity can be monitored and fluorescent probes can be used to study monolayer phases. Also, the re-spreading, which describes whether a surfactant gets depleted from the interface into the subphase with the respiratory cycles, can be obtained with the help of the Wilhelmy balance, as described by Turcotte *et al.*<sup>25</sup>.

### Pulsating bubble surfactometer

The pulsating bubble surfactometer (PBS) is an instrument used to monitor the dynamic surface tension of fluids and requires only micro-litre quantities of sample. It was first described by Enhorning<sup>26</sup>. Figure 4 shows a schematic representation of the PBS. It consists of a sample chamber, a pulsator unit and a pressure-recording device. The sample chamber with a 0.5 mm diameter Teflon tubing is filled with 25 µl of the liquid to be tested. It is turned upside down and is connected by a vertical metal tube to the pulsator and pressure transducer. The chamber and metal tube are surrounded by a thermostat bath filled with water, maintained at 37°C. The volume displacement of the pulsator's mov-

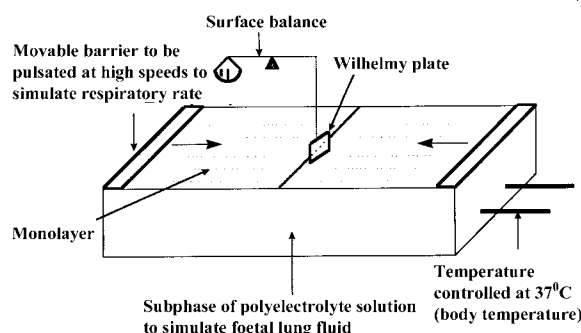


**Figure 3.** Wilhelmy balance modified for application to the lung surfactant system.

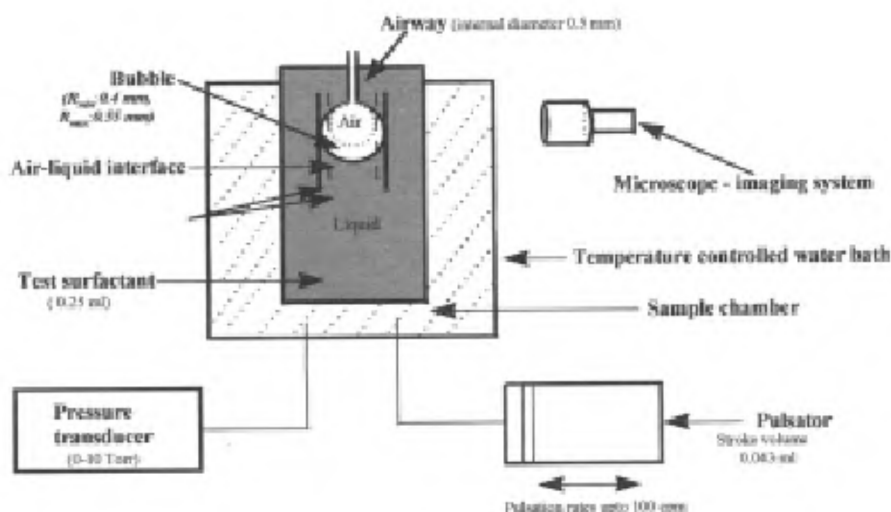


Figure 4. Schematic representation of a pulsating bubble surfactometer.

ing piston is hydraulically geared down 1000 times, which gives the pulsator a stroke volume of 0.43 ml. A syringe withdrawing oil from the hydraulic system is used to create a bubble in the sample chamber. The size of the bubble is checked through a microscope. The pulsating bubble communicates with ambient air. A precision pressure transducer is used to record the pressure across the interface when the bubble is of maximal and minimal size.

The bubble radius changes from a maximum of 0.55 mm to a minimum of 0.4 mm. The pulsator speed can be varied from 0 to 100 cpm. Since the bubble communicates with ambient air, the pressure gradient ( $\Delta P$ ) across the surface of the bubble is the absolute value of the recorded pressure. From the Laplace formula, as it applies for a spherical surface,  $\Delta P = 2\gamma/r$ , the surface tension  $\gamma$  of the sample can be calculated as  $\Delta P$  and  $r$  (radius of the bubble) are measured.

The minimum and maximum surface tension is recorded. Also, the stability of surfactants can be compared by their stability index (SI) which is calculated as  $SI = 2(\gamma_{\max} - \gamma_{\min})/(\gamma_{\max} + \gamma_{\min})$ , where  $\gamma_{\max}$  is the surface tension in the bubble of maximum radius and  $\gamma_{\min}$  the minimum surface tension obtained on pulsation<sup>27</sup>.

#### Advantages and disadvantages

This instrument has the advantages of quick results and the requirement of very small sample volumes (25  $\mu$ l). The bubble can be pulsated at high rates and hence rates corresponding to the respiratory frequency can be used for improved relevance to *in vivo* neonatal respiratory conditions. Contact angle artifacts are avoided and 100% humidity is automatically maintained. The values of minimum and maximum surface tension are easily obtained.

However, there is no way of knowing which components of a surfactant system have been recruited to the air-aqueous interface and in what concentrations. Errors occur at near-zero surface tension values due to defor-

mation of the bubble from a spherical shape. Also, continuity of the monolayer between the bubble and the capillary causes the actual area decrease on compression to be lower than that estimated and creates a path for leakage. The leakage is partly overcome by repeated cycling which progressively fills and compresses the film in the wet capillary, eventually preventing film flow back to the bubble surface such that the capillary acts like a dry one<sup>28</sup>. Important information regarding the surface activity of the first compression film cannot be accurately studied using this instrument.

#### Captive bubble surfactometer

Captive bubble surfactometer (CBS) is a modification of the PBS in which the bubble is not open to the exterior and thus forms a completely spherical interface<sup>29</sup>. In this instrument, pressure changes are used to change the area of a sessile bubble. The captive bubble is floated against a 1% agarose gel and the chamber is sealed and pressurized, thereby decreasing air volume. As the surface area of the bubble is decreased, the surface tension also reduces. The surface tension is calculated by measurements of the height and diameter of the bubble<sup>30-32</sup>. The bubble is completely surrounded by water and hence the molecules of surfactant at the interface cannot escape. Figure 5 shows a schematic representation of a CBS. Figure 6 shows actual photomicrographs of the bubble as it looks at the equilibrium surface tension of 25 mN/m and the functional surface tension of 3 mN/m, as observed with rabbit lung surfactant.

#### Advantages and disadvantages

This instrument overcomes the problem of leakage, which is seen with the PBS and is also more precise in quasi-static and dynamic surface tension determination.

Putz *et al.*<sup>28</sup> compared the performance of surfactants – rabbit lung lavage surfactant, Survanta (an animal-derived therapeutic surfactant) and a synthetic lipid surfactant mixture using both a PBS and a CBS. Both the instruments indicated low surface tension for rabbit lung surfactant at the end of the first cycle itself. However, for Survanta only the CBS reported low surface tension values in the first cycle, whereas the PBS did not achieve low values even after 10 cycles. This indicates that the CBS is more accurate than the PBS. This instrument has been essential in demonstrating the importance of low compressibility as an indicator of effective surfactant function<sup>33</sup>.

### Relevance of surface properties to lung function

The most important parameter of a successful lung surfactant is its ability to lower surface tension at the alveolar air–liquid interface to near-zero values. DPPC has a bulk gel-to-fluid transition of 41.5°C, which is higher for monolayers at a high surface pressure<sup>24</sup>. Thus DPPC monolayers at 37°C are rigid enough to be compressed to very low surface tensions without collapse and are the prime surface-tension lowering component of pulmonary surfactant. Lowering of surface tension during expiration prevents the lungs from collapsing and decreases the work of breathing.

The surfactant monolayer should be stable at low surface tension without collapse. The extreme stability of lung surfactant and DPPC has been demonstrated by the fluorocarbon droplet and captive bubble techniques.

With subsequent breaths, there is a slow collapse and loss of material from the interface. Thus, for adequate functioning replenishment of the surfactant at the interface is important. Replenishment of the surface during film expansion can occur via relaxation of compressed components of the film, adsorption from subphase structures and re-spreading from collapsed and selec-

tively excluded phases. SP-B and SP-C promote adsorption and are probably instrumental in the final transfer of surfactant molecules to the interface. SP-A improves adsorption in the presence of the hydrophobic proteins and could be responsible for moving material near the interface, forming a reservoir and perhaps in the selective insertion of DPPC to the interface<sup>34</sup>.

A low compressibility, as defined by Gaines<sup>35</sup> and applied to the pulmonary surfactant system by King and Clements<sup>36</sup>, is desirable in order to achieve low surface tensions with a minimal area change. If a surfactant with low compressibility is present in the lungs, surface tension will be reduced with very little compression and a large volume of air in the lungs would remain for gas-exchange.

### Surface viscoelasticity

The surface viscoelastic properties of the surfactant films are also of importance but are extremely difficult

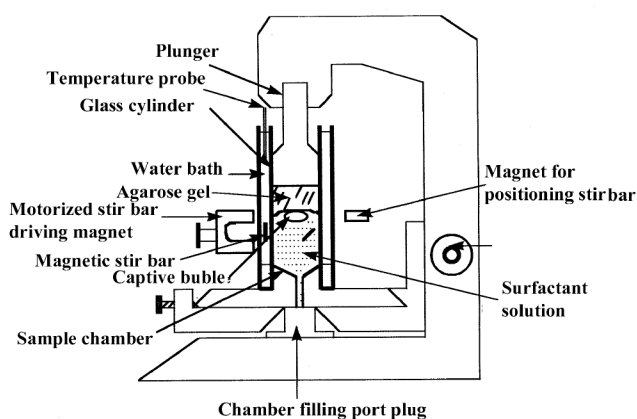


**Figure 5.** Schematic representation of a captive bubble surfactometer (reproduced from Schurch<sup>48</sup>).

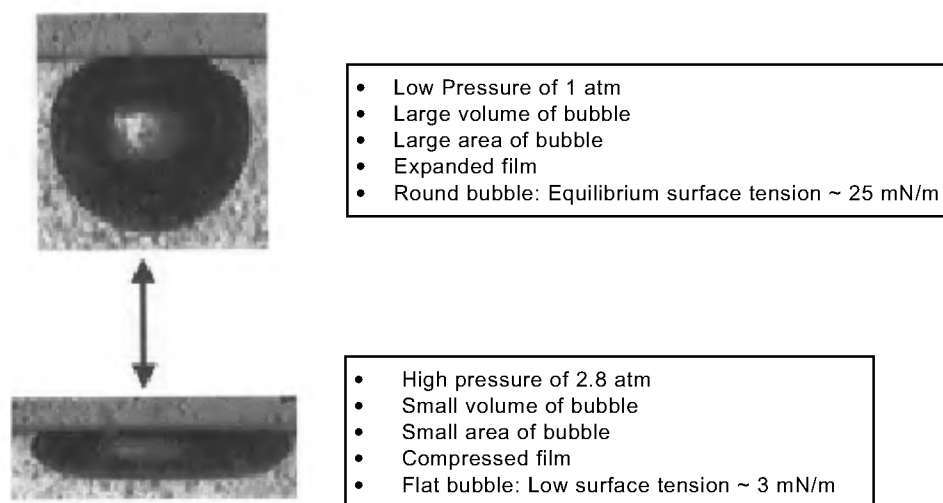


**Figure 6.** Actual photomicrographs of rabbit lung surfactant bubbles at equilibrium and low surface tension.

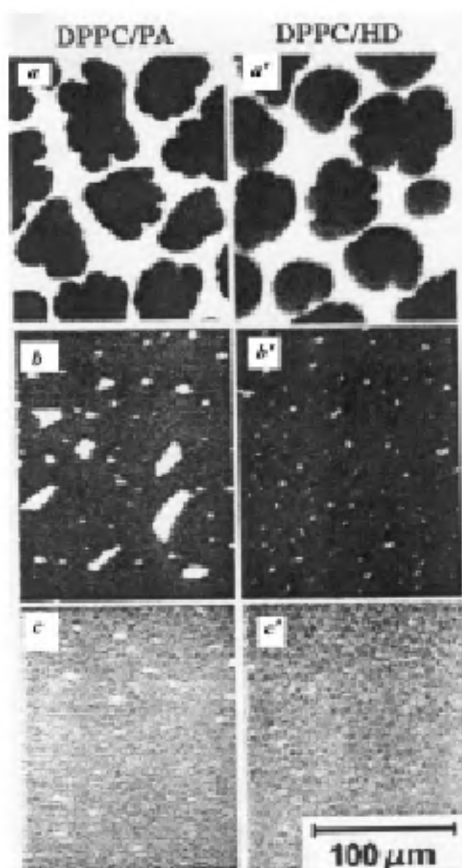


**Figure 7.** Fluorescence images of DPPC/PA and DPPC/hexadecanol mixtures. The ratio of DPPC/PA was in mole ratios (a) 3:1 (b) 1:1 (c) 1:2, and DPPC/HD in mole ratios (a') 3:1 (b') 1:1 (c') 1:2. Images were obtained using BODIPY<sup>®</sup> FL C12 as fluorescence dye. The BODIPY segregates preferentially into disordered regions of the monolayer, rendering liquid-expanded domains bright and condensed regions dark. All images were taken at 30°C on a water subphase and at a lateral pressure of 15 mN/m. The bright liquid-expanded phase is eliminated with increasing fractions of PA or HD in favour of the dark condensed phase. To develop contrast in the FM images, 0.5 mol% of the lipid-analog fluorescent dye, 4,4-difluoro-5,7-dimethyl-4-bora-3a,4a-diaza-s-indacene-3-dodecanoic acid ~BODIPY<sup>®</sup> FL C12, was used. (Reprinted from 'Influence of palmitic acid and hexadecanol of the phase transition temperature and molecular packing of dipalmitoylphosphatidylcholine monolayers at the air–water interface', Lee, K. Y. C., Gopal, A., von Nahmen, A., Zasadzinski, J. A., Majewski, J., Smith, G. S., Howes, P. B. and Kjaer, K., *J. Chem. Phys.*, 2002, **116**, 774–783.)

to characterize experimentally. Surfactant-specific proteins are known to facilitate the spreading of a surfactant monolayer<sup>37</sup>. Pastrana *et al.*<sup>38</sup> have shown that the presence of 1 mol% protein markedly increased the elasticity of surface films, suggesting a mechanism by which SP-C facilitates the spreading of phospholipids on an aqueous surface.

### Fluorocarbon droplet method

Novel experiments by Schurch *et al.*<sup>39</sup> used calibrated fluorocarbon droplets to study the surface tension of the lungs *in vivo*. Droplets of certain fluorocarbon liquids with low surface tensions were calibrated, by their abil-

ity to spread on DPPC monolayers held at different surface tensions. By shape analysis, calibration curves of droplet dimensions and surface tension were made. These droplets were then placed on the alveolar surfaces of cat lungs using micropipettes and surface tension was directly measured at lung volumes ranging from total lung capacity to functional residual capacity.

### Fluorescence microscopy

The phenomenon of fluorescence was known by the middle of the 19th century. Stokes made the observation that the mineral fluorspar fluoresces when ultraviolet light is directed upon it and coined the word 'fluorescence'. Stokes also observed that the fluorescing light has a longer wavelength than that of the excitation light. Fluorescence microscopy is an excellent method for studying material which can be made to fluoresce, either in its natural form (primary or autofluorescence) or when treated with chemicals capable of fluorescing (secondary fluorescence). The basic task of the fluorescence microscope is to permit excitation light to irradiate the specimen and then to separate the much weaker re-radiating fluorescent light from the brighter excitation light. Thus, only the emission light reaches the eye and the resulting fluorescing areas shine against a dark background with sufficient contrast to permit detection.

Fluorescence microscopy techniques have provided visual confirmation that films from surfactant lipids and pulmonary extracts undergo phase transitions during dynamic compression at an air–aqueous interface<sup>40,41</sup>. A commonly used fluorescent probe for mixed lipid films is 1-palmitoyl, 2-nitrobenzoxadiazole amino-dodecanoyl (NBD)-phosphatidylcholine. The gel-like liquid condensed phases (LC) are observed as dark regions due to exclusion of fluorescent probes from such regions against a bright background of liquid expanded phases (LE). This is explained by a less dense packing of the lipids in the LE domains with respect to the LC phase. The interaction between surfactant lipids and proteins can also be studied by this technique using labelled proteins. SP-A binds to the gel-like condensed regions of DPPC<sup>42</sup>. SP-C has been found to alter the packing of molecules in DPPC monolayers, whereas SP-B has not caused perturbations in the lipid monolayers<sup>43,44</sup>. Figure 7 depicts the fluorescence micrographs of DPPC monolayers. This technique reveals useful information, but it is difficult to simulate conditions of body temperature, high compression speed and high humidity. Also, the presence of the probe may cause some changes in the behaviour observed.

### Atomic force microscopy

An atomic force microscope (AFM) consists of scanning a sharp tip on the end of a flexible cantilever

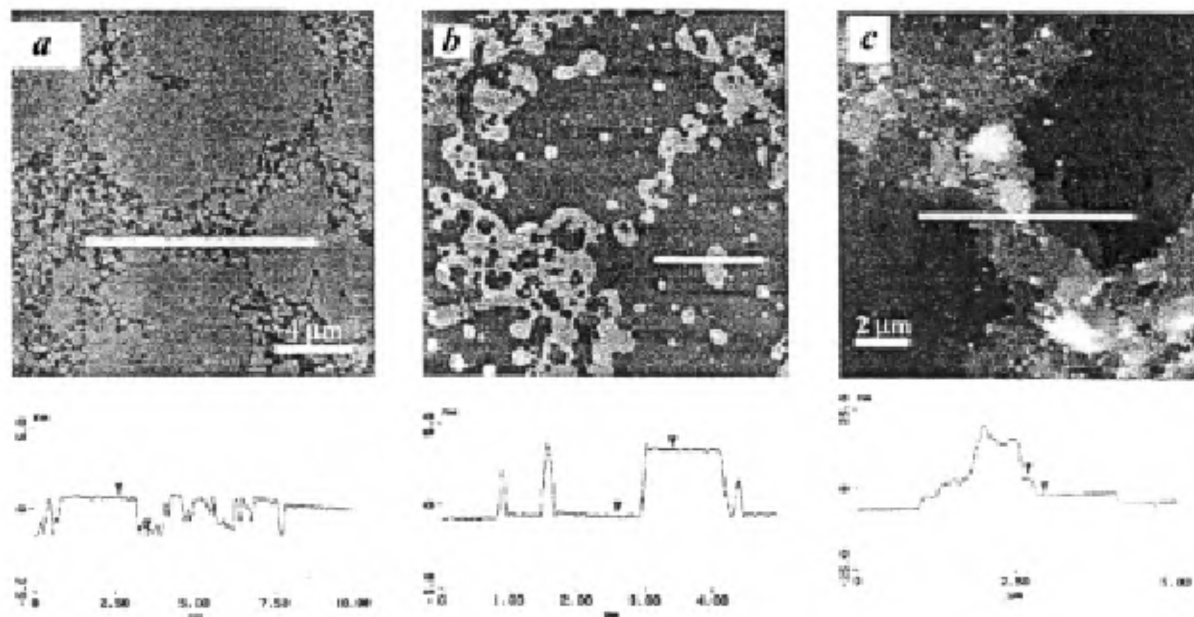


**Figure 8.** AFM images of model lung surfactant monolayers. *a*, Contact mode AFM image of model lung surfactant monolayer (DPPC/POPG/PA/sP-C<sub>ff</sub> in weight ratio of 68:22:8:2) transferred from the air–water interface at a surface pressure 45 mN/m, onto a mica substrate at 30°C. The height trace (white line in image) shows the solid phase domains are 1–2 nm thicker than the fluid phase domains. The solid phase domains consist of all *trans*, extended chains and are expected to be thicker and less compressible than the fluid phase domains, which consist of disordered chains. The irregular shape and 5–10 micron size of the solid phase domains are the same as observed at the air–water interface with fluorescence microscopy; *b*, Contact mode AFM image of the same film (DPPC/POPG/PA/SP-C<sub>ff</sub> in weight ratio of 68:22:8:2) transferred at a surface pressure of 55 mN/m at 30°C, which is above the break in the isotherm. Now, the fluid phase domains are light gray, indicating that the fluid phase is thicker than the solid phase. The height trace (white line in image) shows that the fluid phase is 4 nm higher than the solid phase. This shows that the fluid phase has increased in thickness by 5–6 nm in comparison to (*a*). *c*, AFM image of 3:1 DPPC/POPC, with 2 wt% SP-c<sub>ff</sub> transferred at a surface pressure above the first plateaus in the isotherm at 50 mN/m and 30°C. When the solid phase consists of only DPPC, the fluid phase forms multiplayer steps rather than a uniformly thickened fluid phase (*b*). This stepped morphology is similar to that observed in DPPC/DPPG films with palmitoylated human recombinant SP-C. (Reproduced from ‘Effects of lung surfactant proteins, SP-B and SP-C and palmitic acid on monolayer stability’, Ding, J., Takamoto, D. Y., von Nahmen, A., Lipp, M. M., Lee, K. Y. C., Waring, A. J. and Zasadzinski, J. A., *Biophys. J.*, 2001, **80**, 2262–2272.)

across a sample surface, while maintaining a small constant force. The scanning motion is brought about by a piezoelectric tube scanner, which scans the tip in a raster pattern with respect to the sample (or scans the sample with respect to the tip). The tip–sample interaction is monitored by reflecting a laser off the back of the cantilever into a split photodiode detector. By detecting the difference in the photo detector output voltages, changes in the cantilever deflection or oscillation amplitude are determined. The two most commonly used modes of operation are contact mode and tapping mode, which are conducted in air or liquid environments. Contact mode AFM consists of scanning the probe across a sample surface, while monitoring the change in cantilever deflection with the split photodiode detector. A feedback loop maintains a constant cantilever deflection by vertically moving the scanner to maintain a constant photo detector difference signal. The distance the scanner moves vertically at each data point is stored by the computer to form the topographic image of the sample surface. Tapping mode AFM consists of oscillating the cantilever at its resonance frequency and lightly ‘tapping’ on the surface during scanning. The

laser deflection method is used to detect the root-mean-square amplitude of cantilever oscillation. A feedback loop maintains constant oscillation amplitude by moving the scanner vertically at every data point. The topographic image is formed by recording this movement. The advantage of tapping mode is that it eliminates the lateral shear forces which are present in the contact mode and can thus be used for studying delicate surfaces.

AFM is emerging as a promising tool for investigating the topography of lung surfactant films. DPPC films at high surface tensions have been shown to have an irregular pattern with co-existence of LE and LC phases. At lower surface tension, the films become homogenous with a predominance of the LC phase. This could explain the low compressibility of pure DPPC films at surface tensions lower than 50 mN/m (ref. 45). Evidence from recent studies using AFM have suggested that the traditional concept of a homogenous monolayer lining the lungs may not hold true and that the structure–function relationship may be far more complex. von Nahmen *et al.*<sup>46</sup> have shown SP-C containing surfactant films at tensions ~ 20 mN/m had pro-



trusions of 28 and 77 nm in height, which is compatible with the formation of multilayers. Complex web-like structures were seen on protein-lipid interaction by Amrein *et al.*<sup>47</sup>. An example of the use of AFM in the lung surfactant system is shown in Figure 8. It must be kept in mind that the topology of films as characterized by height differences in AFM, might not reflect the true molecular arrangement and may be influenced by forces between the molecules and the probe, and differences might result also due to transfer onto a mica surface.

## Summary

Lung surfactant reduces the surface tension at the air-liquid interface of the lungs, thereby preventing the alveoli (the smallest respiratory units of the lungs) from collapsing during expiration. Various *in vitro* techniques commonly used in surface science are modified to suit them for application to the lung surfactant system. The ability to form a film rapidly, reach near-zero surface tensions with 15–20% compression, and to be stable over a period of time are some pre-requisites of an optimal surfactant. Our knowledge of this system has improved over the years, but we still have a lot to learn about this complex system. Gene knockout studies and sophisticated microscopic techniques may help clarify many aspects and make us re-think some of our earlier concepts.

1. Veldhuizen, R., Nag, K., Orgeig, S. and Possmayer, F., *Biochim. Biophys. Acta*, 1998, **1408**, 90–108.
2. Jobe, A. H., *Early Hum. Dev.*, 1994, **29**, 283–286.
3. Scarpelli, E. M. and Mautone, A. J., *Biophys. J.*, 1994, **67**, 1080–1089.
4. Clements, J. A., *Physiologist*, 1962, **5**, 11–28.
5. Jobe, A., in *Neonatal Cardiopulmonary Distress* (eds Emmanouilides, G. C. and Baylen, B. G.), Year Book Medical Publishers, Inc, Chicago, 1988, pp. 297–322.
6. Stark, A. R. and Frantz, I. D. III, *Pediatr. Clin. North Am.*, 1986, **33**, 533–544.
7. Tomashefski, J. F. Jr., Vawter, G. F., Reid, L. M., in *Pulmonary Development: Transition from Intrauterine to Extrauterine Life* (ed. Nelson, G. H.), Marcel Dekker, Inc, New York, 1985, pp. 387–429.
8. Richman, P. S., Batcher, S. and Catanzaro, A., *J. Lab. Clin. Med.*, 1990, **116**, 18–26.
9. Kurashima, K., Ogawa, H., Ohka, T., Fujimura, M., Matsuda, T. and Koyabashi, T., *Arerugi*, 1991, **40**, 160–163.
10. Anzueto, A. *et al.*, *J. Am. Med. Assoc.*, 1997, **278**, 1426–1431.
11. Erokhin, V. V. and Lepekha, L. N., *Vestn. Rossiiskoi Akad. Med. Nauk*, 2000, **12**, 31–36.
12. Xie, E., Yang, Z. and Li, A., *Zhonghua Wai Ke Za Zhi, Chin. J. Surg.*, 1997, **35**, 745–748.
13. Subramaniam, S., Whitsett, J. A., Hull, W. and Gairola, C. G., *Toxicol. Appl. Pharmacol.*, 1996, **140**, 274–280.
14. Muller, B., Seifart, C. and Barth, P. J., *Eur. J. Clin. Invest.*, 1998, **28**, 762–777.
15. Khyshiktuev, B. S. and Ivanov, V. N., *Pathophysiology*, 1998, **5**, 143.
16. Clements, J. A., *Proc. Exp. Biol. Med.*, 1957, **93**, 170–172.

17. Nielson, D. W., *J. Appl. Physiol.*, 1986, **60**, 972–979.
18. Mautone, A. J., Reilly, K. E. and Mendelsohn, R., *Biochim. Biophys. Acta*, 1987, **896**, 1–10.
19. Seeger, W., Stohr, G., Wolf, H. R. D. and Neuhoof, H., *J. Appl. Physiol.*, 1985, **58**, 326–338.
20. Tabak, S. A. and Notter, R. H., *J. Colloid Interface Sci.*, 1977, **59**, 293–300.
21. Morley, C. J., Bangham, A. D., Miller, N. and Davis, J. A., *Lancet*, 1981, **i**, 64–68.
22. Phillips, M. C. and Chapman, D., *Biochim. Biophys. Acta*, 1968, **163**, 301–313.
23. Hills, B. A., in *The Biology of Surfactant*, Cambridge University Press, Cambridge, 1988, pp. 167–168.
24. Goerke, J. and Gonzales, J., *J. Appl. Physiol.*, 1981, **51**, 1108–1114.
25. Turcotte, J. G., Sacco, A. M., Steim, J. M., Tabak, S. A. and Notter, R. H., *Biochim. Biophys. Acta*, 1977, **488**, 235–248.
26. Enhorning, G., *J. Appl. Physiol.*, 1977, **43**, 198–203.
27. Clements, J. A., Hustead, R. F., Johnson, R. P. and Gribetz, I., *J. Appl. Physiol.*, 1961, **16**, 444–450.
28. Putz, G., Goerke, J., Tauesch, H. W. and Clements, J. A., *ibid*, 1994, **76**, 1425–1431.
29. Schurch, S., Qanbar, R., Bachofen, H. and Possmayer, F., *Biol. Neonate*, 1995, **67**, 61–76.
30. Malcolm, J. D. and Elliott, C. D., *Can. J. Chem. Eng.*, 1980, **58**, 151–153.
31. Schurch, S., Bachofen, H., Goerke, J. and Possmayer, F., *J. Appl. Physiol.*, 1989, **67**, 2389–2396.
32. Schoel, W. M., Schurch, S. and Goerke, J., *Biochim. Biophys. Acta*, 1994, **1200**, 281–290.
33. Schurch, S., Schurch, D., Curstedt, T. and Robertson, B., *J. Appl. Physiol.*, 1994, **263**, 974–986.
34. Perez-Gil, J. and Keough, K. M. W., *Biochim. Biophys. Acta*, 1998, **1408**, 203–217.
35. Gaines, G. L. Jr., *Insoluble Monolayers at Liquid-Gas Interfaces*, Interscience Publishers, New York, 1966.
36. King, R. J. and Clements, J. A., *Am. J. Physiol.*, 1972, **223**, 715–733.
37. Taneva, S. and Keough, K. M. W., *Biochemistry*, 1997, **36**, 912–922.
38. Pastrana, B., Mautone, A. J. and Mendelsohn, R., *Biochemistry*, 1991, **30**, 10058–10064.
39. Schurch, S., Goerke, J. and Clements, J. A., *Proc. Natl. Acad. Sci. USA*, 1976, **73**, 4698–4702.
40. Nag, K., Perez-Gil, J., Ruano, M. L. F., Worthman, L. D., Stewart, J., Casals C. and Keough K. M. W., *Biophys. J.*, 1998, **74**, 2983–2985.
41. Discher, B. M., Maloney, K. M., Schief, W. R. Jr., Grainger, D. W., Vogel, V. and Hall, S. B., *Biophys. J.*, 1996, **71**, 2583–2590.
42. Ruano, M. L., Nag, K., Worthman, L. A., Casals, C., Perez-Gil, J. and Keough, K. M., *Biophys. J.*, 1998, **74**, 1101–1109.
43. Lipp, M. M., Lee, K. Y. C., Zasadzinski, J. A. and Waring, A. J., *Science*, 1996, **273**, 1196–1200.
44. Nag, K., Taneva, S. G., Perez-Gil, J., Cruz A. and Keough, K. M., *Biophys. J.*, 1997, **72**, 2638–2650.
45. Grunder, R., Gehr, P., Bachofen, H., Schurch, S. and Siegenthaler, H., *Eur. Respir. J.*, 1999, **14**, 1290–1296.
46. von Nahmen, A., Schenk, M., Sieber, M. and Amrein, M., *Biophys. J.*, 1997, **72**, 463–469.
47. Amrein, M., von Nahmen, A. and Sieber, M., *ibid*, 1997, **26**, 349–357.
48. Schurch, S., *Clin. Perinatal*, 1993, **20**, 669–682.
49. Panaiotov, I., Ivanova, Tz., Proust, J., Boury, F., Denizot, B., Keough K. and Taneva, S., *Colloids Surf. B: Biointerfaces*, 1996, **6**, 243–260.

Received 29 November 2000; revised accepted 9 November 2001